

# Monolayer-functionalized microfluidics devices for optical sensing of acidity

P. Mela,<sup>†ab</sup> S. Onclin,<sup>†c</sup> M. H. Goedbloed,<sup>a</sup> S. Levi,<sup>b</sup> M. F. García-Parajó,<sup>b</sup> N. F. van Hulst,<sup>\*b</sup> B. J. Ravoo,<sup>c</sup> D. N. Reinhoudt<sup>\*c</sup> and A. van den Berg<sup>\*a</sup>

Received 1st July 2004, Accepted 9th November 2004

First published as an Advance Article on the web 26th November 2004

DOI: 10.1039/b409978h

This paper describes the integration of opto-chemosensors in microfluidics networks. Our technique exploits the internal surface of the network as a platform to build a sensing system by coating the surface with a self-assembled monolayer and subsequently binding a fluorescent sensing molecule to the monolayer. Fluorescent molecules were used that can switch between a fluorescent and a non-fluorescent state, depending on the acidity of the surrounding solution. Two systems were investigated. The first employs surface confinement of a Rhodamine B dye in a glass micro channel that serves as a molecular switch in organic solutions. Upon rinsing the micro channels with acidic or basic solutions it was possible to switch between the fluorescent and non-fluorescent forms reversibly. Moreover, this system could be used to monitor the mixing of two solutions of different acidity along the micro channel. To widen the scope of optical sensing in micro channels an Oregon Green dye derivative was immobilized, which functions as a sensing molecule for pH differences in aqueous solutions. In this case, a hybrid system was used consisting of a glass slide and PDMS channels. The fluorescence intensity was found to be directly correlated to the pH of the solution in contact, indicating the possibility of using such a system as a pH sensor. These systems allow real-time measurements and can be easily implemented in micro- and nanofluidics systems thus enabling analysis of extremely small sample volumes in a fast and reproducible manner.

## Introduction

In many fields the advances in fabrication technology have led to a reduction in size of devices by several orders of magnitude. One area that benefits in particular from this trend is the area of micro total analysis systems ( $\mu$ TAS), also called “lab on a chip”.<sup>1</sup> Microfabricated systems are of great current interest in biological and life sciences for the analysis of biological macromolecules,<sup>2,3</sup> as well as for the development of sensors and chemical synthesis on-chip.<sup>4</sup> Microfluidics devices are characterized by a high surface-to-volume ratio: surface effects become dominant in fluid handling and surface properties play a crucial role in chip-based applications. One straightforward method to generate modified surfaces is by using self-assembled monolayers (SAMs). Deposition of SAMs is amenable to implementation in microfluidics devices, since it only requires the flow of a solution or a gas stream of adsorbate molecules through the channels. Many of the microfluidics systems are based on glass or silicon, implying that trichloro- or trialkoxysilane derivatives can be employed for surface modification. SAMs have been used in glass microfluidics networks to engineer surface properties with the aim of controlling liquid motions,<sup>5</sup> confining and aligning of biological macromolecules and liquid crystals,<sup>6,7</sup> stabilizing the

liquid interface in an extraction system,<sup>8</sup> controlling electro-osmotic flow,<sup>9,10</sup> preventing cell adhesion<sup>10,11</sup> and protein adsorption,<sup>12</sup> and creating zones for specific immobilization of proteins.<sup>13</sup>

When derivatized with fluorescent groups, SAMs can function as optical sensors. This has been shown on flat surfaces,<sup>14–17</sup> and also in microfluidics networks.<sup>17,18</sup> This paper describes the immobilization of two molecular switches in a microfluidics device. Molecular switches are systems capable of reversible interconversion between two or more states.<sup>19,20</sup> Among the different families of switches, chemically driven switches are especially interesting for applications in sensing and biology,<sup>21,22</sup> and have even been studied at a single molecule level.<sup>23,24</sup> Immobilization of such a molecular switch in a microfluidics network could potentially be used to probe solutions inside the microfluidics network, to monitor processes inside the channel, or to control processes in the channel.

The first part of this paper describes the surface confinement of a molecular switch in a glass microfluidics network by attaching it to a monolayer. The molecular switch interconverts between a fluorescent and non-fluorescent state, based on the acidity of the organic solution that is in contact with the monolayer. To demonstrate the wide scope of this methodology, a second molecular switch is immobilized, which is able to sense differences in pH of *aqueous* solutions by a change in fluorescence response. In this case, a hybrid microfluidics system, consisting of glass and PDMS, is

<sup>†</sup> Both authors contributed equally to this work.

\*n.f.vanhulst@utwente.nl (N. F. van Hulst)

smct@utwente.nl (D. N. Reinhoudt)

a.vandenberg@utwente.nl (A. van den Berg)

employed. PDMS networks represent a useful alternative for the fabrication of microfluidics devices. They are easy to fabricate, transparent in the UV-vis region, chemically inert, compatible with aqueous solutions,<sup>25</sup> and have a low cost of fabrication.<sup>26</sup> In addition, PDMS shows a strong adhesion to glass surfaces, allowing easy assembly of such hybrid systems.

## Experimental

### General procedures

All moisture-sensitive reactions were carried out under nitrogen or argon atmosphere. Reagents are commercially available and were used without further purification, unless stated otherwise. Toluene was distilled from Na, and methylene chloride was purified over active aluminium oxide and stored over molecular sieves. <sup>1</sup>H NMR spectra were recorded at 25 °C using a Varian Inova 300 spectrometer. <sup>1</sup>H NMR chemical shifts (300 MHz) are given relative to residual CHCl<sub>3</sub> (7.25 ppm). FAB-MS spectra were recorded on a Finnigan Mat 90 spectrometer with *m*-nitrobenzylalcohol as a matrix.

### Materials and methods

All glassware used to prepare monolayers and to perform subsequent reactions was cleaned by immersing in a piranha solution (H<sub>2</sub>SO<sub>4</sub> (96%) : H<sub>2</sub>O<sub>2</sub> (30%) 3 : 1 v/v). **Cautions:** piranha is a very strong oxidant and reacts violently with many organic materials. Subsequently, the glassware was rinsed with large amounts of Millipore water and dried in an oven.

### Rhodamine B acid chloride

Rhodamine B (laser grade) (50 mg, 0.104 mmol) was dissolved in 10 ml of dry methylene chloride. A large excess of oxalyl chloride (3 ml) was added to the solution, and the reaction mixture was stirred under argon for 30 min at room temperature. The color of the reaction mixture changed from red to purple. The solvent was evaporated under reduced pressure. The excess of oxalyl chloride was removed by evaporating with a vacuum pump. The obtained purple solid was used without further purification.

### Rhodamine B propylamine

Rhodamine B acid chloride was dissolved in 20 ml of dry methylene chloride. Subsequently, 10 equivalents of propylamine were added (61 mg, 1.04 mmol) and the reaction mixture was stirred overnight. The solvent and propylamine were evaporated under reduced pressure. The remaining solid was taken up in dichloromethane and washed with 0.1 N HCl, brine and water. The solvent was removed under reduced pressure to give Rhodamine B propylamine as a pink solid (47 mg, 0.091 mmol, 87%). <sup>1</sup>H NMR (CDCl<sub>3</sub>): δ 7.91 (m, ArH, 1H), 7.43 (m, ArH, 2H), 7.09 (m, ArH, 1H), 6.26–6.48 (m, ArH, 6H), 3.36 (q, 8H, NCH<sub>2</sub>CH<sub>3</sub>), 3.12 (t, 2H, NCH<sub>2</sub>CH<sub>2</sub>), 1.58 (m, 2H, CH<sub>2</sub>CH<sub>2</sub>CH<sub>3</sub>), 1.19 (t, 12H, CH<sub>2</sub>CH<sub>3</sub>), 0.71 (t, 3H, CH<sub>2</sub>CH<sub>3</sub>); MS (FAB): *m/z* calcd for M–Cl<sup>+</sup> 484.3; found 484.3.

### Substrate preparation

The inside of microfluidics channels, glass slides, and silicon wafers were cleaned in boiling piranha for 15 min, rinsed with copious amounts of Millipore water and dried in a stream of nitrogen.

### Monolayer preparation and surface reactions

**Coupling of RhB to APTES monolayers.** Cleaned channels or silicon wafers were placed in a dry glove box and brought in contact with a 0.25% (v/v) solution of APTES in freshly distilled toluene at room temperature for 2.5 h, after which they were rinsed extensively with toluene and methylene chloride. Finally they were dried in a stream of nitrogen. The functionalized glass substrates were brought in contact with a 10<sup>−6</sup> M solution of RhB acid chloride in methylene chloride, containing a 10-fold excess of acetyl chloride, for 1.5 h at room temperature. Acetyl chloride was used as a non-fluorescent competitive reagent to limit the number of fluorescent RhB molecules that are linked to the NH<sub>2</sub>-functionalized glass surface. After anchoring RhB acid chloride and acetyl chloride to the surface *via* amide formation, the substrates were rinsed extensively with methylene chloride and ethanol and finally dried in a stream of nitrogen.

Amino monolayers from 1-cyano-11-trichlorosilylundecane: This procedure has been reported previously.<sup>27</sup>

**Coupling of Oregon Green 514 succinimidyl ester to amino SAMs, and subsequent capping.** Oregon Green 514 carboxylic acid, succinimidyl ester (OG 514, Molecular Probes, Inc. Eugene, OR USA) was covalently coupled to the amino SAMs by immersion of the substrates in a 10<sup>−5</sup> M solution of OG 514 in acetonitrile containing 0.05 ml of diisopropylethylamine (DIPEA) for 2.5 h at room temperature. After attachment, the substrates were rinsed and sonicated in acetonitrile and chloroform and dried in a stream of nitrogen. The remaining free amines were capped by immersing the substrates in a solution containing 0.1 ml of butyl isothiocyanate and 0.05 ml of DIPEA in acetonitrile for 2.5 h at room temperature. Finally, the glass slides were rinsed and sonicated in acetonitrile and chloroform and dried in a stream of nitrogen.

### UV-vis spectroscopy

UV-vis spectroscopy was performed on a Hewlett Packard 8452A diode array spectrophotometer using quartz sample cells of 10 mm. UV-vis measurements were performed in 10<sup>−5</sup> M methylene chloride solutions.

### Laser scanning confocal microscopy

The confocal set up used for detection of the fluorescent signals is a home-built set up based on a Zeiss Axiovert 135 TV microscope. The microscope is equipped with a home-built scanning stage (80 × 80 μm<sup>2</sup> maximal scan area). Light from an Ar : Kr laser (Spectra Physics, BeamLok 2060) has been used in the experiments ( $\lambda_{\text{exc}}$  = 514.4 nm). Circularly polarized light has been achieved with a combination of a  $\lambda/2$  and a  $\lambda/4$  wave plate. The beam is then coupled into the

back aperture of a  $63 \times$  Olympus 1.4 NA immersion oil objective *via* a dichroic mirror (Omega 540DRLP) and focused onto the bottom surface of the channel. The fluorescence emitted from the illuminated volume is separated from the residual excitation light by using a rejection band filter (514.5 Raman) directed onto two glass fibers that serve as pinholes and sent to two avalanche photo diodes (SPCM-AQ-14, EG&G Electro Optics). Fluorescence data recording was performed using an interface card *PCI-MIO-16E4* (National Instruments, USA) and software written in *LabVIEW 6.1* (National Instruments, USA). Areas of  $70 \times 70$  and  $40 \times 40 \mu\text{m}^2$  were scanned. Each scan area consisted of  $256 \times 256$  pixels, photons were collected for 1 ms on each pixel, the excitation power was within the range  $0.05\text{--}0.15 \text{ kW cm}^{-2}$ . Post-processing of the data was also done with software written in *LabVIEW*.

### Microfluidics network fabrication

**Glass networks.** Microchips were fabricated with conventional wet-etch technology at MESA<sup>+</sup> cleanroom facilities. One side of a 1.1 mm thick Borofloat glass wafer (SCHOTT GLAS, Mainz Germany) was covered with a  $0.7 \mu\text{m}$  thick amorphous silicon (a-Si) layer by means of Plasma Enhanced Chemical Vapor Deposition (PECVD). A layer of photoresist Olin907/17 (Olin Microelectronic Materials Norwalk, CT, USA) was spin-coated on top of the a-Si layer and patterned to act as mask for the Reactive Ion Etching (RIE) of the a-Si layer which served then as a mask for the etching of the channels in the glass substrate. Etching for 12 min in a 10% HF solution resulted in  $2 \mu\text{m}$  deep channels. Access holes to the channels were made in the same substrate by powder blasting. The wafer was then cleaned in acetone by ultrasound and subsequently in fuming  $\text{HNO}_3$ . The a-Si layer was dissolved in KOH. After rinsing in DI-water and drying, the wafer was fusion-bonded to a  $0.5 \text{ mm}$  thick Pyrex wafer (Pyrex<sup>®</sup> 7740, Corning, NY, USA). The Pyrex wafer was then thinned down to  $170 \mu\text{m}$  (required for the confocal microscope) by HF etching, while protecting the Borofloat side with dicing foil.

**PDMS networks.** The PDMS micro channels were fabricated using a replica molding method on a silicon wafer patterned by conventional lithography. First the silicon wafer was spun with Ti35 SE image reversal photoresist (Olin Microelectronic Materials Norwalk, CT, USA), and exposed

through the same mask used for the glass network fabrication. After development, the resist patterned a network on the silicon surface. The silicon was then etched to a depth of  $2 \mu\text{m}$  with Reactive Ion Etching (RIE) using  $\text{SF}_6$  plasma ( $12 \text{ sccm SF}_6$ ,  $50 \text{ mTorr}$ ,  $75 \text{ Watt}$ ). The photoresist was stripped in acetone, and the silicon surface spin-coated with a fluorocarbon solution (1 : 1 FC40 : FC722, 3M Netherlands, Leiden, NL) to prevent the PDMS from sticking to the silicon. PDMS prepolymer and curing agent (Sylgard 184, Dow Corning) were mixed in a 10 : 1 ratio (v/v), degassed under vacuum, poured onto the master, and cured at  $80 \text{ }^\circ\text{C}$  for 2 h. The PDMS replica was then carefully peeled off.

Both fabrication techniques resulted in chips with outer dimensions of  $15 \times 20 \text{ mm}^2$ . Each chip fits inside a Delrin custom-made holder (Dupont) onto which tubing is connected to create pressure driven flows. In the base of the holder, magnets are placed in order to fix the holder on a stainless steel platform mounted on the scanning stage of the confocal microscope and guarantee in this way a fixed relative position between the chip and the objective.

## Results and discussion

### A Rhodamine B molecular switch

Rhodamine B (RhB) derivatives containing primary amide groups at the 2'-position can be switched reversibly between a fluorescent amide form and a non-fluorescent spirolactam upon addition of acid or base.<sup>28</sup> A molecular switch (shown in Fig. 1) was synthesized in two steps from RhB. First, RhB was reacted with oxalyl chloride to yield RhB acid chloride, which was subsequently reacted with propylamine to give **1** in 87% yield. Upon addition of base, **1a** converts to its lactam form causing interruption of the electron resonance in the dye. Upon acid addition, the amide moiety in **1b** is protonated and **1a** is formed by opening of the lactam. This reaction results in the recovery of the aromaticity of the system. The UV-vis spectrum in Fig. 1 clearly shows the difference in absorbance for the two species.

Titration of small amounts of acetic acid to a diluted solution of **1b** results in a marked increase of the fluorescence. Fig. 2 shows the titration curve for additions of 1 to 25% of acetic acid to a  $10^{-6} \text{ M}$  RhB lactam solution. The system is sensitive enough to detect the addition of 1% of acetic acid and reaches maximum fluorescence intensity after addition of *ca.* 20% of acetic acid.

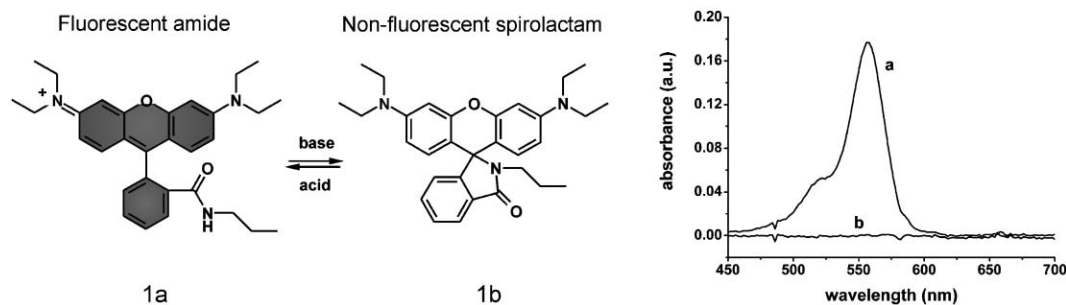


**Fig. 1** Molecular structures of the RhB-derivatized molecular switch and corresponding UV-vis spectra of a  $10^{-5} \text{ M}$  solution of **1** in methylene chloride.

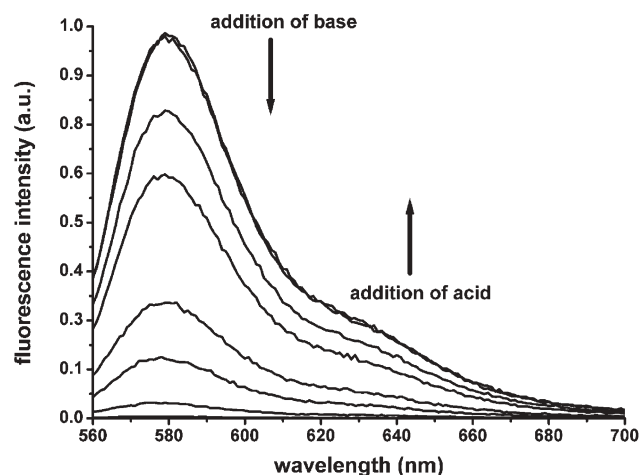
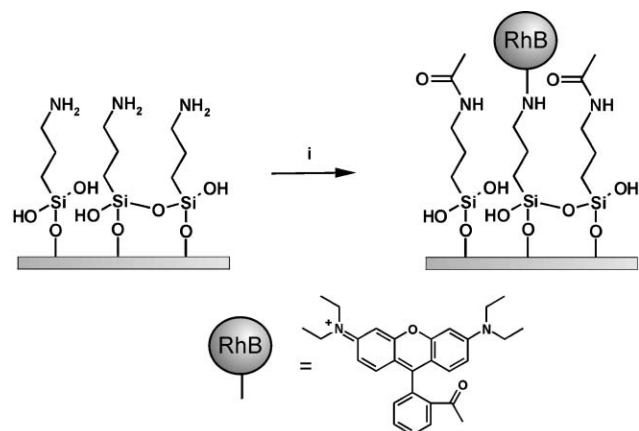


**Fig. 2** Emission spectra of **1** in methylene chloride as a function of added acetic acid. Shown spectra contain 1, 3, 5, 10, 15, 20, and 25% of acetic acid. Addition of triethylamine results in quenching of the fluorescence (data not shown).

### Immobilization of the RhB switch

RhB was attached to the SiO<sub>2</sub> surface through reaction with a preformed amino monolayer. RhB was first activated by reaction with oxalyl chloride, generating the acid chloride derivative, which can be used to react with the amino monolayer. To limit the number of attached dye molecules to the surface and simultaneously cap the remaining free amines, the reaction was performed in the presence of a 10-fold excess of a non-fluorescent competitive reagent, acetyl chloride. The process is schematically shown in Scheme 1.

The procedure to immobilize the RhB molecules was performed on planar silicon wafers and in micro channels. The planar substrates were used to characterize the monolayer formation and subsequent reaction. Exposing the cleaned substrates to a toluene solution containing 3-aminopropyl triethoxysilane (APTES) resulted in an ellipsometric thickness of 0.6 nm and an advancing contact angle of 63°, corresponding to an amino-terminated monolayer.<sup>29</sup> After reaction with



**Scheme 1** Immobilization of the RhB molecular switch on a preformed amino SAM and capping of the remaining free amines: (i) RhB acid chloride, acetyl chloride, methylene chloride.

RhB acid chloride and acetyl chloride the ellipsometric thickness increased to 1.2 nm and the advancing contact angle to 69°, indicating a successful surface attachment.

### Optical sensing of acidity inside a micro channel

Functionalization of the glass surface and subsequent immobilization of RhB inside the microfluidics network was performed by pumping the reagents by means of syringes. A schematic representation of the chip and the network layout is depicted in Fig. 3A. All reagents were introduced at reservoir 4. After functionalization with APTES, the channels were rinsed extensively using pressure driven flows of methylene chloride and ethanol to remove physisorbed material from the walls of the microfluidics network. Subsequently, a solution containing RhB acid chloride and acetyl chloride was flowed through the channels, after which the channels were rinsed extensively with methylene chloride. The fluorescence responses of the sensing molecules were monitored by mounting the microfluidics network on a laser scanning confocal microscope (LSCM). Fig. 3B shows an example of the fluorescence signal of the RhB monolayer after inspection with an LSCM, and the mean fluorescence intensity measured over 10 line scans. The microfluidics channel is clearly visible and the emitted fluorescence appeared to be uniform throughout the whole device. The enhanced fluorescence intensity at the edges of the channel can be explained by the presence of RhB molecules on the sidewalls of the channel.

To verify if the surface-confined RhB is able to switch in a similar manner as the solution counterpart, a fixed area of the network (70 × 70 μm<sup>2</sup>) was inspected with LSCM while flowing acidic and basic solutions through the channels. Solvents were fed into channels 1 and 2 by means of syringes. Channels 3 and 4 were used as outlets. A flow of acetic acid in methylene chloride (20% v/v) was pumped into the network *via* inlets 1 and 2 by pressure and the fluorescence intensity of the layer was recorded (Fig. 4, scan 1). Subsequently, a solution of triethylamine in methylene chloride (20% v/v) was flowed through the channels and the same area of the network was imaged again (Fig. 4, scan 2). The fluorescence intensity was reduced to approximately 30% of the intensity under acidic conditions, implying that fluorescent molecules were converted from the fluorescent amide form to the non-fluorescent spirolactam form. The fact less than 100% decrease in fluorescence intensity was observed might be caused by steric constraints of the immobilized dyes in the monolayer. The RhB dye must change its conformation to form the spirolactam. In addition, the high local concentration of dye molecules could result in energy transfer processes that change the fluorescence properties. Reintroducing the acidic solution at inlet 2 showed that the switching process is reversible: the fluorescence emission of the RhB molecules was completely recovered (Fig. 4, scan 3). Employing the laminar flow of fluids inside microfluidics networks allowed studying the mixing of fluids of different acidity along the micro channel. Introducing the triethylamine solution at inlet 1 and the acetic acid solution at inlet 2 gave a clear gradient in fluorescence intensity across the channel width, representing the difference



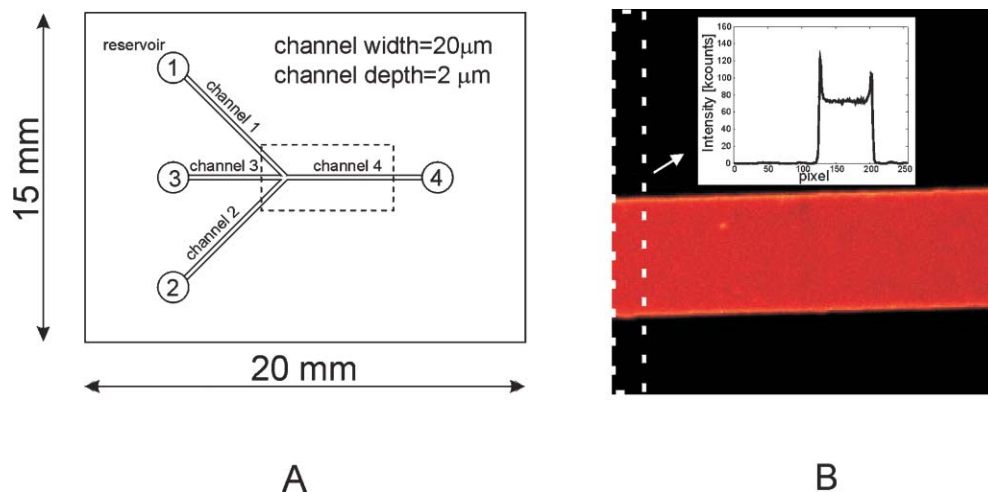


**Fig. 3** (A) Schematic representation of chip layout. The dotted rectangle corresponds to the area inspected with confocal microscopy. (B) Typical confocal microscopy image ( $70 \times 70 \mu\text{m}^2$ ) and mean fluorescence intensity (inset) measured over 10 scan lines.

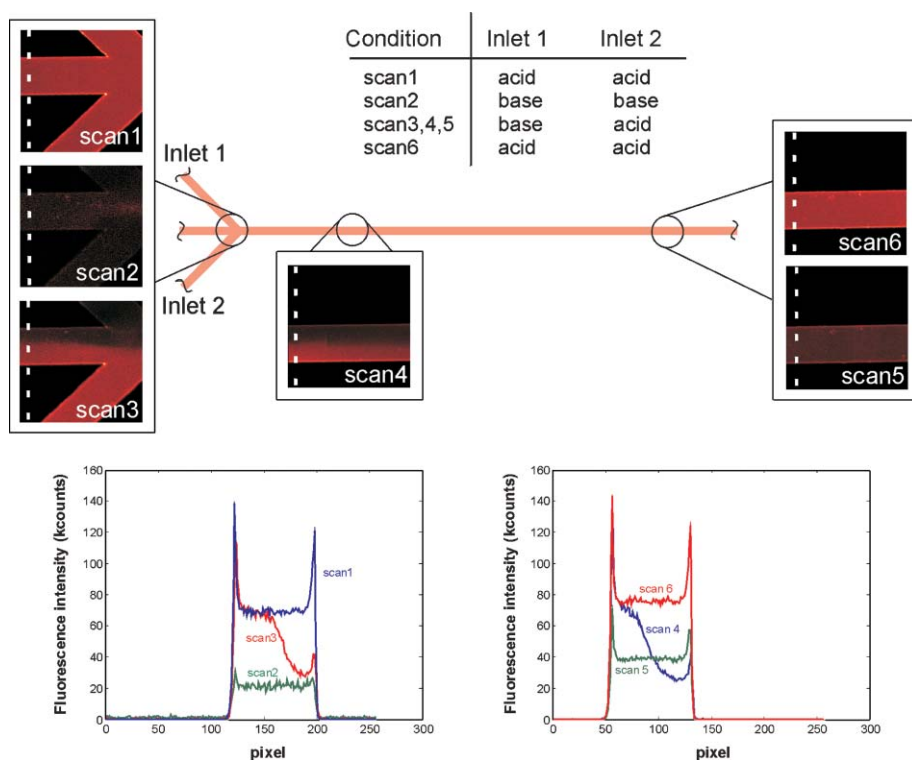


**Fig. 4** Confocal microscopy images of the RhB-functionalized microfluidics chip at different positions along the channel, using various conditions (see Table), and mean fluorescence intensity profiles for each scan averaged over 10 scan lines.

in acidity of both solutions (Fig. 4, scan 3). The effect of diffusion-controlled mixing could be monitored along the micro channel towards outlet 4 (Fig. 4, scan 4), and at a more downstream position the fluorescence intensity of the solution was found to be uniform across the channel width, indicating complete mixing of the two fluids (Fig. 4, scan 5). Both solutions are 20% in volume, which means that more acetic acid molecules than triethylamine molecules are present in solution, accounting for the observed fluorescence intensity.<sup>30</sup> Replacing the base in reservoir 1 with the acidic solution created the starting conditions again, and the emission of the layer was fully recovered (Fig. 4, scan 6).

The reproducibility and stability of the fluorescence signal were further tested by repeated acid/base cycles over a time period of 5.5 h. The normalized fluorescence intensity values are depicted in Fig. 5 and demonstrate that the system is stable over this time period. The immobilized RhB molecules respond to changes in acidity with a clear and reproducible change in fluorescence emission.

The possibility of autofluorescence causing the observed changes in fluorescence intensity was ruled out by performing control experiments in a microfluidics network without functionalized monolayer. The channels were cleaned with the same procedure used prior to functionalization, and acidic and

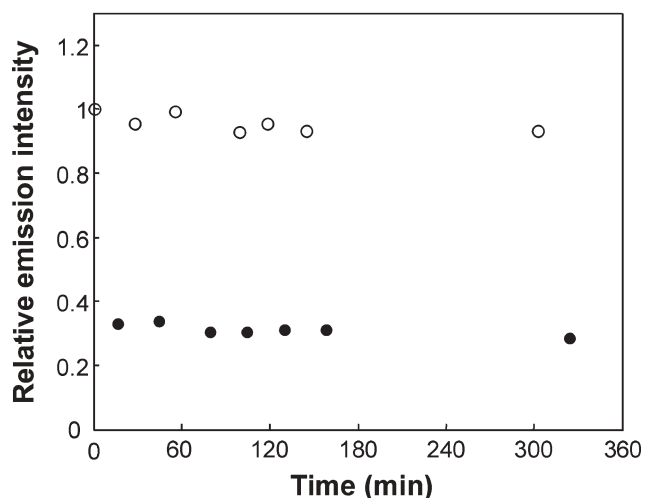


**Fig. 5** Repeated on–off switching of the RhB molecules in the microfluidics channel. Relative mean fluorescence intensity after alternating exposure to acid (open dots) and to base (solid dots). In between acid–base cycles the channels were rinsed with methylene chloride.

basic solutions were alternatively flowed through the channels. The measured autofluorescence of the solvents was *ca.* three orders of magnitude lower than the fluorescence detected in RhB-functionalized channels using the same solvents.

Thus, the surface-confined fluorophores are able to sense the acidity of the surrounding solution in a similar manner as their

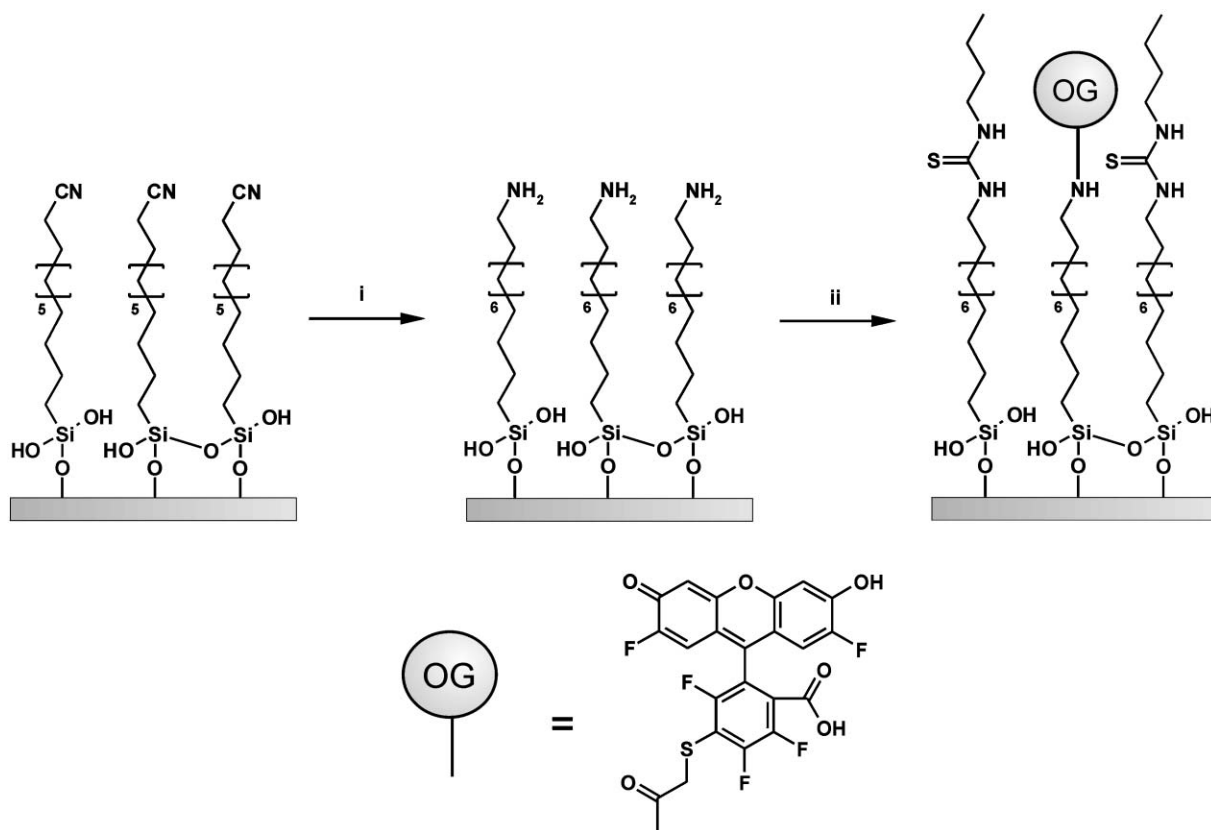
solution counterparts. The detection limit of this system was not explored, as these are proof of principle experiments, but is likely to be dependent on the sensitivity of the confocal microscope.

#### pH sensing in aqueous solution

To widen the scope of optical sensing from organic solutions to aqueous solutions, a second molecule was immobilized that displays pH-dependent fluorescence.<sup>31</sup> Oregon Green dyes are fluorinated analogs of fluoresceins and are considered to be better pH sensors than fluorescein because of their greater photostability.<sup>32</sup> One application of this probe is to trace the pH in different cellular compartments.<sup>33</sup>

Here, a functionalized derivative of Oregon Green 514 (OG514) is immobilized onto a preformed monolayer to sense the pH of solutions in microfluidics networks. Instead of using glass-fabricated networks a hybrid system, consisting of a microscope glass slide and a poly(dimethylsiloxane) (PDMS) stamp, was employed.

To attach OG514 to a monolayer, the succinimidyl ester derivative was reacted with a preformed amino SAM, after which the remaining free amines were capped by reaction with butyl isothiocyanate. The procedure is shown schematically in Scheme 2. For this system a monolayer containing a long alkyl chain was employed instead of APTES, as APTES monolayers display only a limited stability in aqueous solution, which is probably caused by the absence



**Scheme 2** Immobilization of the OG514 molecular switch on a preformed amino SAM, followed by capping of the remaining free amines: (i) Red Al, toluene, 40 °C; (ii) (a) OG514 succinimidyl ester, diisopropylethylamine, acetonitrile; (b) butyl isothiocyanate, diisopropylethylamine, acetonitrile.

of well-defined structure in the siloxane networks of this difunctional reagent.<sup>34</sup>

Our procedure to prepare water stable amino SAMs has been reported previously.<sup>27</sup> First, a cyano-terminated monolayer is prepared from 1-cyano-11-trichlorosilylundecane, which is subsequently reduced to the corresponding amine. The advancing contact angle of the amino monolayer was  $61^\circ$  and had an ellipsometric thickness of 2.0 nm. After attachment of OG514, followed by capping of the remaining free amines with butyl isothiocyanate, the advancing contact angle increased to  $74^\circ$  and the ellipsometric thickness to 2.7 nm, indicative of a successful surface attachment.

Micro channels fabricated in PDMS and monolayer-modified microscope glass slides were placed in a custom-made holder onto which tubing was connected for pressure driven flows. A schematic representation of the hybrid system is depicted in Fig. 6. The bonding between PDMS and the glass was not very strong, probably due to the presence of the sensing layer, but allowed the flowing of aqueous solutions through the channels. A possible solution for this problem could be found in the use of epoxy glue to seal the two components of the device.<sup>35</sup>

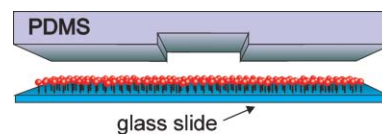


**Fig. 6** Schematic representation of hybrid microfluidics system: a PDMS stamp on top of a monolayer-modified microscope glass slide.

The microfluidics system was flushed with four aqueous solutions of different pH value in a random order. Fig. 7A shows LSCM images of a fixed area ( $40 \times 40 \mu\text{m}^2$ ) of the micro channel when flowing the four different solutions through the channel. It is evident that the fluorescence intensity depends on the pH of the solution. Fig. 7B depicts the relative fluorescence intensity as a function of the pH of the solution. The measured data (solid points) were fitted to a sigmoidal curve (solid line), and from this curve a  $pK_a$  value was obtained of *ca.* 4.9, which matches the reported  $pK_a$  value of 4.8 for OG514 in aqueous solution.<sup>33,36</sup> Sensitivity in different pH regimes can be easily obtained by tailoring the glass surface with other pH dependent dyes, demonstrating the wide applicability of this approach.

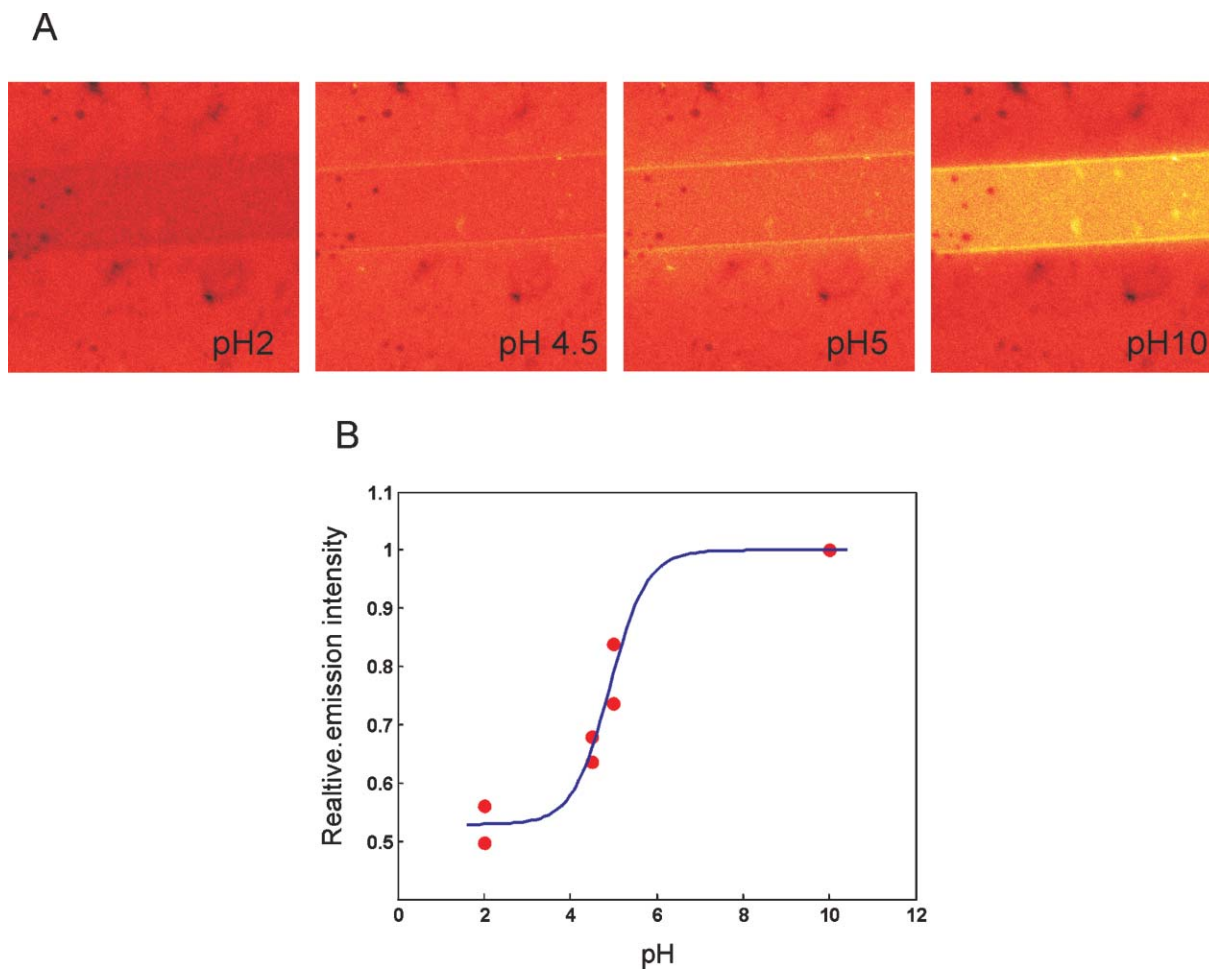


**Fig. 7** (A) Confocal microscopy images ( $40 \times 40 \mu\text{m}^2$ ) of a PDMS channel on the functionalized microscope glass slide at four different pH values. (B) Relative emission intensities as a function of pH value: experimental data (solid dots) obtained from the OG514 functionalized layers and fitted curve (solid line).

The observed increase in fluorescence intensity of a factor two upon going from acidic to basic pH values is modest when compared to similar measurements in solution,<sup>36</sup> but this behavior has been observed before for immobilized Oregon Green dyes.<sup>37</sup> Immobilization results in a high local concentration of dye molecules, which could result in energy transfer processes that change the fluorescence properties of OG514. In addition, part of the dye molecules might be buried within the hydrophobic alkyl chains of the monolayer, rendering them inaccessible to the aqueous solution and therefore unable to switch between the fluorescent and non-fluorescent forms.

## Conclusions

Monolayers bearing fluorescent groups that are able to sense changes in acidity of the surrounding solution have been immobilized in microfluidics devices. Rhodamine B-derivatized monolayers were confined to the walls of glass-fabricated micro channels and were able to switch between a fluorescent and a non-fluorescent state reversibly, depending on the acidity of the organic solution inside the micro channel. In addition, a hybrid system, consisting of glass and PDMS, was employed to attach Oregon Green 514 to the glass surface. This system was able to sense the pH of aqueous solutions that flowed through the fluidics network by a change in fluorescent properties.

This approach of immobilizing sensing molecules inside microfluidics networks could find widespread application for monitoring processes inside a fluidics network. The main advantage of using fluorescence spectroscopy as an analysis tool is that integration with analysis equipment is not necessary, enabling real-time monitoring of processes inside the fluidics network. The benefit of using SAMs to confine the sensing molecules is their ease of preparation and the short response times, since the sensing molecules are in direct contact with the medium to be analyzed.

## Acknowledgements

This project was supported through the Microchemical Systems Program (MiCS) of the MESA<sup>+</sup> Institute for Nanotechnology.

P. Mela,<sup>†ab</sup> S. Onclin,<sup>†c</sup> M. H. Goedbloed,<sup>a</sup> S. Levi,<sup>b</sup> M. F. Garcia-Parajo,<sup>b</sup> N. F. van Hulst,<sup>\*b</sup> B. J. Ravoo,<sup>c</sup> D. N. Reinhoudt<sup>\*c</sup> and A. van den Berg<sup>\*a</sup>

<sup>a</sup>BIOS Group, MESA<sup>+</sup> Institute for Nanotechnology, University of Twente, P.O. Box 17, 7500 AE Enschede, The Netherlands. E-mail: a.vandenberg@utwente.nl

<sup>b</sup>Applied Optics Group, MESA<sup>+</sup> Institute for Nanotechnology, University of Twente, P.O. Box 217, 7500 AE Enschede, The Netherlands. E-mail: n.f.vanhulst@utwente.nl

<sup>c</sup>Supramolecular Chemistry and Technology, MESA<sup>+</sup> Institute for Nanotechnology, University of Twente, P.O. Box 217, 7500 AE Enschede, The Netherlands. E-mail: smct@utwente.nl

## References

1 D. J. Harrison, K. Fluri, K. Seiler, Z. H. Fan, C. S. Effenhauser and A. Manz, *Science*, 1993, **261**, 895–897.

- 2 D. R. Reyes, D. Iossifidis, P. A. Auroux and A. Manz, *Anal. Chem.*, 2002, **74**, 2623–2636.
- 3 P. A. Auroux, D. Iossifidis, D. R. Reyes and A. Manz, *Anal. Chem.*, 2002, **74**, 2637–2652.
- 4 X. Z. Feng, S. J. Haswell and P. Watts, *Curr. Top. Med. Chem.*, 2004, **4**, 707–727.
- 5 B. Zhao, J. S. Moore and D. J. Beebe, *Science*, 2001, **291**, 1023–1026.
- 6 Y. Li, T. Pfohl, J. H. Kim, M. Yasa, Z. Wen, M. W. Kim and C. R. Safinya, *Biomed. Microdevices*, 2001, **3**, 239–244.
- 7 T. Pfohl, J. H. Kim, M. Yasa, H. P. Miller, G. C. L. Wong, F. Bringezu, Z. Wen, L. Wilson, M. W. Kim, Y. Li and C. R. Safinya, *Langmuir*, 2001, **17**, 5343–5351.
- 8 A. Hibara, M. Nonaka, H. Hisamoto, K. Uchiyama, Y. Kikutani, M. Tokeshi and T. Kitamori, *Anal. Chem.*, 2002, **74**, 1724–1728.
- 9 Z. J. Sui and J. B. Schlenoff, *Langmuir*, 2003, **19**, 7829–7831.
- 10 B. J. Kirby, A. R. Wheeler, R. N. Zare, J. A. Fruetel and T. J. Shepodd, *Lab Chip*, 2003, **3**, 5–10.
- 11 J. D. Cox, M. S. Curry, S. K. Skirboll, P. L. Gourley and D. Y. Sasaki, *Biomaterials*, 2002, **23**, 929–935.
- 12 N. J. Munro, A. F. R. Huhmer and J. P. Landers, *Anal. Chem.*, 2001, **73**, 1784–1794.
- 13 L. Xiong and F. E. Regnier, *J. Chromatogr., A*, 2001, **924**, 165–176.
- 14 S. Flink, F. C. J. M. van Veggel and D. N. Reinhoudt, *Adv. Mater.*, 2000, **12**, 1315–1328.
- 15 N. J. van der Veen, S. Flink, M. A. Deij, R. J. M. Egberink, F. C. J. M. van Veggel and D. N. Reinhoudt, *J. Am. Chem. Soc.*, 2000, **122**, 6112–6113.
- 16 M. Crego-Calama and D. N. Reinhoudt, *Adv. Mater.*, 2001, **13**, 1171–1174.
- 17 L. Basabe-Desmonts, J. Beld, R. S. Zimmerman, J. Hernando, P. Mela, M. F. Garcia Parajo, N. F. Van Hulst, A. van den Berg, D. N. Reinhoudt and M. Crego-Calama, *J. Am. Chem. Soc.*, 2004, **126**, 7293–7299.
- 18 C. M. Rudzinski, A. M. Young and D. G. Nocera, *J. Am. Chem. Soc.*, 2002, **124**, 1723–1727.
- 19 J.-M. Lehn, *Supramolecular Chemistry, Concepts and Perspectives*, Wiley VCH, Weinheim, 1995.
- 20 V. Balzani, M. Gomez-Lopez and J. F. Stoddart, *Acc. Chem. Res.*, 1998, **31**, 405–414.
- 21 A. E. Stellwagen and N. L. Craig, *Trends Biochem. Sci.*, 1998, **23**, 486–490.
- 22 B. J. Coe, *Chem.–Eur. J.*, 1999, **5**, 2464–2471.
- 23 S. Brasselet and W. Moerner, *Single Mol.*, 2000, **1**, 17–23.
- 24 S. Levi, *Supramolecular Chemistry at the Nanometer Level*, PhD Thesis, University of Twente, Enschede, The Netherlands, 2001.
- 25 J. N. Lee, C. Park and G. M. Whitesides, *Anal. Chem.*, 2003, **75**, 6544–6554.
- 26 J. M. K. Ng, I. Gitlin, A. D. Stroock and G. M. Whitesides, *Electrophoresis*, 2002, **23**, 3461–3473.
- 27 S. Onclin, A. Mulder, J. Huskens, B. J. Ravoo and D. N. Reinhoudt, *Langmuir*, 2004, **20**, 5460–5466.
- 28 M. Adamczyk and J. Grote, *Bioorg. Med. Chem. Lett.*, 2000, **10**, 1539–1541.
- 29 S. Flink, *Sensing monolayers on gold and glass*, PhD Thesis, University of Twente, Enschede, The Netherlands, 2000.
- 30 Both solutions are 20% in volume, which means that 2.4 times more acetic acid molecules are present.
- 31 The RhB molecule discussed in the ‘sensing acidity in organic solution’ section does not switch in aqueous solution.
- 32 R. P. Haugland, *Handbook of fluorescent probes and research products, ninth edition*, Molecular Probes, Eugene, OR, 2002.
- 33 H. J. Lin, H. Szmazinski and J. R. Lakowicz, *Anal. Biochem.*, 1999, **269**, 162–167.
- 34 M. T. Lee and G. S. Ferguson, *Langmuir*, 2001, **17**, 762–767.
- 35 S. F. Li and S. C. Chen, *IEEE Trans. Adv. Packag.*, 2003, **26**, 242–247.
- 36 C. Delmotte and A. Delmas, *Bioorg. Med. Chem. Lett.*, 1999, **9**, 2989–2994.
- 37 J. Ji, N. Rosenzweig, C. Griffin and Z. Rosenzweig, *Anal. Chem.*, 2000, **72**, 3497–3503.